Growth-front instabilities in solid-state recrystallization of amorphous GaAs films

C. Licoppe and Y. I. Nissim
Laboratoire de Bagneux, Centre National d'Etudes des Télécommunications, 196 Avenue Henri Ravera, 92220 Bagneux, France

C. d'Anterroches
Centre National d'Etudes des Télécommunications, Boîte Postale 98, Chemin du Vieux Chêne, F-38243 Meylan Cedex, France
(Received 30 June 1987)

Results of the observation of growth-front morphologies during solid-state recrystallization of implanted amorphous GaAs are reported. Discrete growth at small length scales and continuous instabilities at large length scales are simultaneously observed for the first time in the solid phase. In the initial stages of recrystallization, the growth front is made of a rough pattern of recrystallized material on the scale of 10–15 Å. In a later stage, parabolic instabilities of the growth front appear. The interface roughness increases as the square root of the recrystallized thickness. This dependence is obtained by *in situ* optical reflectivity experiments. Diffusion of defects in the amorphous layer together with defect reaction at the interface are shown to support well the new experimental data.

Physics of interfacial morphologies in off-equilibrium processes is a rapidly evolving field. Two classes of physical approach may basically be distinguished. Continuous models deal with patterned growth on a relatively large scale, usually over 1000 Å. They have proved to be powerful in studying growth-front instabilities at the melt interface[1] or viscous fingering in porous media.[2] On the other hand, discrete models describing various forms of particulate growth, such as random surface recrystallization in the Eden model and its generalizations,[3,4] diffusion-limited aggregation (DLA),[5–7] and vapor deposition,[8,9] concentrate on interface roughness and fractal dimension, taking into account all length scales down to the size of aggregating particles, which in certain experiments may be microscopic.[10–12] A theoretical attempt to connect the two types of approach has shown that the addition of surface tension to the DLA model leads to dendritic shapes.[13] On the experimental side, such a crossover between aggregative shapes and dendritic growth was observed in Zn electrodeposition, depending on experimental control parameters.[14,15]

This paper reports the observation of such phenomena in a purely solid-phase situation. Recently, a dense branching morphology falling in the category of continuous instabilities was seen to develop during recrystallization of amorphous Al-Ge alloys[16] and discrete fractal growth in recrystallization of amorphous $GeSe_2$.[17] It will be shown in this work that discrete growth and continuous diffusive instabilities can be observed simultaneously since their length scales are not too far apart, thus leading to new interfacial morphologies with mixed features. These results stem from the first direct observation of the growth front at intermediate stages of recrystallization of an implanted GaAs substrate. During recrystallization of amorphous materials, an off-equilibrium disordered structure recovers its crystalline order by a solid-phase transformation, most usually through random nucleation plus subsequent growth. In this context, the study of growth-front morphologies has been hampered by polycrystallization, which multiplies the grains and limits their final size. A technique such as ion implantation has allowed the preparation of thin amorphous films on undamaged crystalline substrates. In such implanted films of Si or GaAs, growth occurs by solid-phase epitaxy (SPE),[18,19] offering a unique opportunity to study interface morphology in solid-state crystallization of amorphous materials. While the growth front has been shown to remain planar during recrystallization of implanted ⟨100⟩-oriented silicon substrates, with a width not exceeding a few tens of angstroms,[20] SPE recrystallization of implanted III-V materials has remained a puzzle. The growth front has been shown to widen up to hundreds of angstroms, independently of the nature of the implanted ions.[21] There is no existing model to describe the phenomenology of SPE recrystallization in III-V materials.

OBSERVATION OF THE INTERFACE BY HIGH-RESOLUTION ELECTRON MICROSCOPY

In our experiments, samples are semi-insulating GaAs wafers implanted with As^+ ions at energies 190, 110, and 40 keV, and doses 8×10^{14}, 2×10^{14}, and 1.3×10^{14} at./cm^2, respectively. This multi-implantation scheme provides a flat implantation profile. It leads to amorphous layers 900 Å thick, as demonstrated by cross-sectional electron microscopy. These samples were partially recrystallized using a limited-time heat treatment at 300 °C. In sample A regrowth was stopped after 300 Å while in sample B it was stopped after 600 Å.

Figure 1 is a typical high-resolution electron microscopy (HREM) micrograph of sample A, focusing on the structure of the interfacial layer. It proves that the GaAs amorphous structure turns abruptly into the crystalline structure, without any intermediate layer; this region is abrupt on the scale of one or two interatomic dis-

 ©1988 The American Physical Society

FIG. 1. HREM micrograph of the growth front after recrystallization of ~300 Å, showing the arborescent grain structure of the interface HREM micrograph.

tances. It also shows a very rough fine structure with connected patches consisting of small crystalline grains of typical size 10–15 Å. These connected grains have the same orientation as the crystalline substrate. It must be noted that amorphous valleys in these arborescent structures show a trend toward ⟨111⟩ orientation. Also, stacking-fault bundles, appearing as dark rectangular bars in Fig. 1, occur preferentially in bulklike recrystallized areas rather than in branching protrusions. The transition region where amorphous and crystalline material are interwoven is approximately 120 Å.

Figure 2 is a typical cross-section HREM micrograph of sample B, at a later stage of recrystallization. It shows that the interfacial structure has evolved into dense continuous recrystallized protrusions oriented in the ⟨111⟩ direction. These structures appear smooth at large scales. Inside these protrusions, a herringbone pattern indicates the presence of stacking faults. At small scales, the interface exhibits less roughness than at the earlier stage of recrystallization of sample A.

One can locate the position of the interface between amorphous and crystalline material by following (111) planes which are a signature of the crystal and which are visible in HREM, up to the point where they disappear. At that point the amorphous material, which appears in HREM as a disordered pattern of dots, starts. The crystalline continuous deformation protruding on the right of Fig. 2 has been delineated in such a way. This provides the interface shape drawn for explanatory purposes in Fig. 3(a). In the several micrographs taken in the course of this study which show such continuous protrusions, these were in all cases oriented along ⟨111⟩ directions. The central axis of the protrusion is then defined as the (111) plane in which direction the crystal reaches the farthest into the amorphous material. Taking the central axis as the ordinate axis, and the abscissa axis as a perpendicular to the central axis in the plane of the picture, one obtains a Cartesian coordinate plot of the shape of the crystalline protusion. In Fig. 3(b) this shape is represented in an (x^2,y) parabolic plot instead of an (x,y) Cartesian one. The linearity observed shows that the protrusion is parabolic on each side of its central axis. It is slightly asymmetric with a curvature radius smaller on the inward side than on the outward side. The crude procedure which has been employed certainly neglects important effects in interface location determination, such as corrections due to the two-dimensional projection of a three-dimensional rough interface. Nevertheless it yields orders of magnitude for curvatures, 50 Å in the inward side and 70 Å on the outward side, which will be convenient for the purposes of this work. This radius is in the same order of magnitude as the size of the structure (150 Å).

Such scales are typical of the observations which were made in the course of this work. Crystalline anisotropy is clearly operating here since protrusions developing along ⟨111⟩ directions are systematically selected. Also, stacking-fault bundles in the same [111] direction are

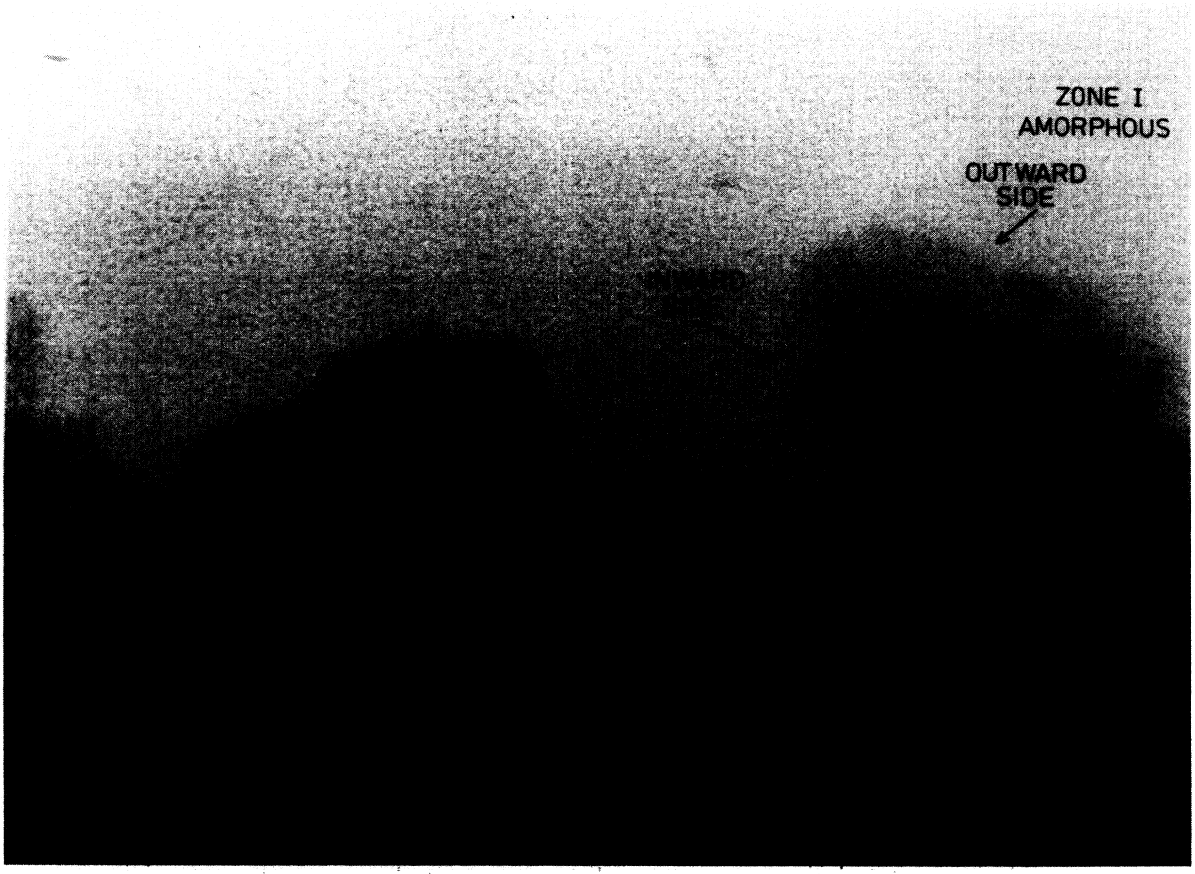

FIG. 2. HREM micrograph of the growth front after recrystallization of ~600 Å, showing nascent large-scale deformations protruding in [111] directions.

seen to accumulate in the crystalline protrusions. It has been shown in previous work that as the interface proceeds towards the surface, roughness increases all the time.[21] Then the deformations of the interface observed here are still at an early stage of development and must keep on evolving with ongoing recrystallization.

In summary, from these micrographs, the recrystallization front goes through two stages: a first stage where local reorganization on a scale of 10–15 Å takes place on a seemingly random basis, leading to a very rough, fuzzy growth front, and a second where the growth front evolves into a pattern of large-size continuous deformations, roughly parabolic in shape.

OPTICAL STUDIES OF THE EPITAXIAL GROWTH-FRONT ROUGHNESS

In this section we will try to use the time-resolved reflectivity (TRR) results to secure quantitative data on interface roughness. If the reflectivity is monitored during solid-phase epitaxial recrystallization of an implanted semiconductor, a characteristic interference modulation is obtained as the epitaxial growth front proceeds toward the surface.[22] Extrema of the reflectivity occur at integer multiple values of $\lambda/4n$ where λ is the probe beam wavelength and n is the optical index of the amorphous material. Provided the interface is less rough than $\lambda/2n$, this allows a determination of the mean position of the growth front.[21]

A previous study showed that the amplitude of the last oscillation in the TRR signal depended only on the initial thickness of the amorphous layer.[21] As the amorphous layer is made thicker, the modulation amplitude decreases. This effect was explained in terms of interfacial nonplanarity. Such an explanation finds a striking confirmation in the HREM data on the interfacial structure displayed in this paper.

Reference 21 describes in detail a numerical simulation of these experimental effects. The interface is modeled by an array of independent columns. The rms height variation of the columns is a measure of the statistical roughness of such a stepped interface. The random height of the interface is then introduced in the Fabry-Perot reflectivity formula.[22] It includes a random-phase factor which causes attenuation of the modulation in a way similar to the experiments.[21] Increasing the mean position of the interface, z, by a given increment and computing the reflectivity at position z provides a numerical simulation of the reflectivity behavior during a regrowth event.

In this work a test initial amorphous depth of 1000 Å has been chosen. Two types of numerical simulations of the reflectivity signal were made. In the first type the roughness was kept at a given value during the simulation. In the second case, its evolution was a linear increase with interface location during the simulation. Figure 4 plots the amplitude of the last oscillation as a

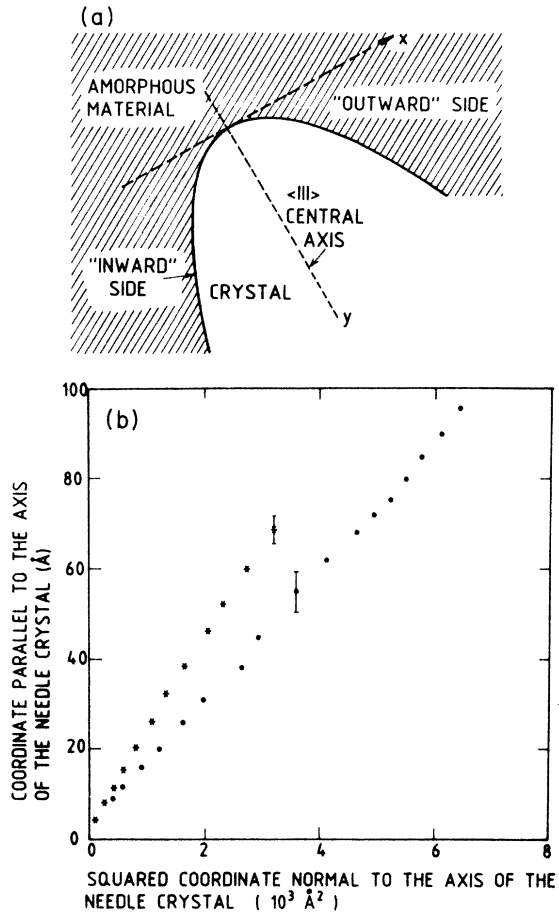

FIG. 3. (a) Schematic drawing of the shape of a crystalline protrusion and of the system of axes used to plot it in Cartesian coordinates. (b) Shape analysis of the most developed crystalline protrusion in HREM micrograph of Fig. 2. Asterisks correspond to the side of the needle crystal making an acute angle with the (100) plane (inward side). Dots correspond to the obtuse angle side of the needle, relatively to (100) orientation (outward side). The slope on the inward side corresponds to a curvature radius ~50 Å; on the outward side it is ~70 Å. Error bars are figured on each curve for clarity.

function of interfacial roughness in both cases. Provided the roughness is less than 200 Å, and the roughness increases linearly with z, the amplitude is insensitive to the precise evolution law of the interface roughness.

Two assumptions have been made in this derivation. The choice of a columnar interface neglects the effect of overhangs in the interfacial profile. Light scattering at the rough interface which also contributes to an attenuation of the interference modulation has been neglected. In our computations the influence of interfacial roughness on interference modulation is then underestimated. Nevertheless, for such an empirically elusive parameter as interface roughness, our indirect definition is a relevant tool for characterizing interface structure.

Coming back to experiments, a determination of the amplitude of modulation in the reflectivity signal was obtained as a function of interface position z.[21] By numerical simulations, we were able to relate the amplitude of modulation to a suitable definition of interface roughness in a geometrical model of the interface. It is then possible to obtain a one-to-one correspondence between the interfacial roughness and the mean position of the interface. This is done in Fig. 5, which shows that the interface-roughness evolution fits well a sublinear power law:

$$\zeta \sim z^{0.5\pm0.05} ,$$

where ζ is the interface roughness and z the mean position of the interface. It must be pointed out that the lower points in Fig. 5 correspond to the situation of the HREM picture in Fig. 1, while the upper points relate to the HREM picture of Fig. 2. Since they all fit the same power-law dependence, this is a strong indication that the transition from a rough discrete pattern at the interface toward continuous large-scale parabolalike deformations is due to a single regrowth mechanism.

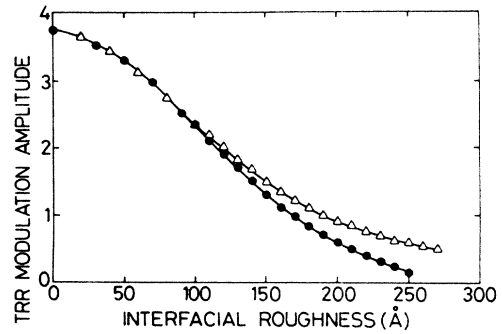

FIG. 4. Numerical simulation results plotting reflectivity interference amplitude (in arbitrary units) as a function of interfacial roughness. The latter comes from a simulation by a statistically-independent-columns model of the rough interface. Open triangles correspond to the case of a constant roughness during interface motion. Test wavelength is taken to be 6328 Å. The curves do not separate significantly before roughness reaches 200 Å.

DISCUSSION

Finding a power law with an exponent near 0.5 for the growth-front roughness is hardly an amazing result. A

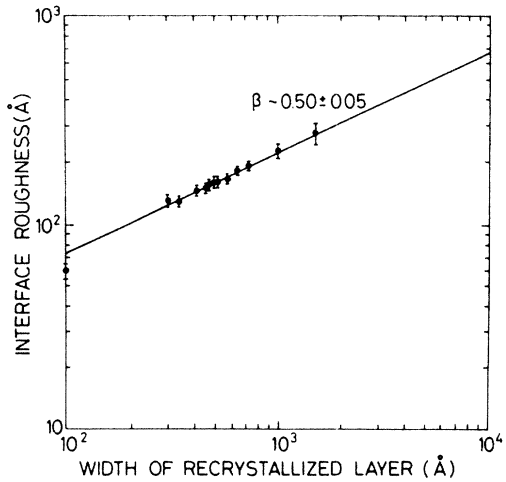

FIG. 5. Interface roughness as a function of recrystallized width.

completely random growth of independent columns exhibits such a power-law dependence. But HREM observations have provided evidence for a patterned growth with parabolic deformations of the growth front in privileged crystalline orientations which calls for a highly correlated behavior. In this section, we will attempt to provide a basis for the understanding of the nature of the correlations which can lead to the experimentally observed interface pattern during regrowth.

In the early stages of recrystallization as pictured in Fig. 1 a treelike pattern is seen to appear at the interface. This has been interpreted as a multiplication of small-scale local reorganization events (LRE's). A typical LRE is the reorganization of a group of atoms of size 10 Å, sitting on the interface, which turns from amorphous to crystalline state. A type of regrowth occurring by a discrete separate LRE at the interface suggests that a comparison with the classic models of discrete aggregation growth could be both relevant and fruitful. If we assume the LRE's to occur on a strictly random basis at the interface, interfacial structure should be related to the behavior of the theoretical Eden model for growth,[3] where the particle is replaced by the group of atoms which goes crystalline. Numerical simulations have provided a dependence of the surface with ζ with the recrystallized thickness z in the form $\zeta \sim z^{0.1}$.[23] An even slower dependence $\zeta \sim \ln z$ has also been suggested.[24] Thorough analysis of the optical reflectivity experiments described in the previous section has yielded $\zeta \sim z^{0.5}$. This is much faster than what the Eden model predicts. Then the LRE's do not occur on a completely random basis at the interface. Another interesting model in this respect is the diffusion-limited aggregation (DLA) (Ref. 5) in which new particles are added to the growing cluster through a random-walk diffusion process. It predicts $\zeta \sim z$.[8] In this limit, the branching and screening effects due to bulk diffusion are overemphasized: growth occurs in the maximum aggregation probability zones. It provides a growth front which roughens faster than the solid-phase epitaxial growth front in GaAs.

At this stage we will define our basic hypothesis. Some kind of diffusion intervenes in the recrystallization process. Such an hypothesis cannot be unambiguously deduced from the new data we have provided. Nevertheless we aim to show that it provides a framework which nicely supports our experiments. The whole assumption is the following: something diffuses in the bulk of the amorphous layer. We will try to define later what the diffusing species can be. This bulk diffusion allows for the volume change and strain relief which is inherent to the crystallization phenomenon. Occurrence of the necessary mass diffusion process ahead of the growth front causes an increased probability of the LRE in the vicinity of the interface. Basically this leads to a picture in which the LRE, which is the aggregating unit in our case, has a probability of occurrence which varys with the diffusion-controlled strain relief behind and ahead of the growth front, on a spatial scale which is that of strain fluctuations. If the characteristic diffusion scale is higher than the LRE size and smaller than a macroscopic cutoff, one obtains a type of growth which stands as an intermediate between DLA growth, that is pure diffusion-limited growth, and Eden growth, that is pure surface reaction limited growth. "Intermediate" is not meant here in the sense of a crossover between the two types of growth, which would lead to a distribution of characteristic exponents and is thus ruled out by the optical experiments, but in the sense of a single type of growth whose constitutive features incorporate ingredients from both models. In its own *ad hoc* way, with a diffusion scale that acts as a parameter, it can account for an intermediate power law $\xi \sim z^{0.5}$.

Combination of surface reaction plus bulk diffusion in the amorphous phase accounts for two distinctive effects observed in SPE recrystallization of implanted semiconductors. Surface reaction should be orientation dependent and it should cause the interfacial structure to depend on substrate orientation. Indeed, this is the case in GaAs (Ref. 25) and InP.[26] Bulk diffusion in the amorphous phase is expected to depend little on substrate orientation, whatever diffuses. On the other hand, surface reaction alone cannot account for the relaxation of extra volume and strain relief in the implanted layer during recrystallization.[27] This volume change can readily be explained if one assumes that microscopic voids in excess are diffusing away from the growth front, or conversely that missing mass is diffusing toward the growth front, during recrystallization. Such a crude picture can only be understood as an average over many different microscopic configurations. Defects in the recrystallized layers, such as unannealed point defects[26] and stacking faults, should also play a part in the strain relief accompanying the recrystallization. However, in conclusion, both bulk diffusion and surface reaction are needed to account for the features of SPE recrystallization. Previously, in studies of silicon, attention has been mostly paid to the substrate orientation effect and thus to regrowth mechanisms mediated by migration of defects on the interface.[28,29]

The presence of diffusion in the amorphous phase finds further support in our HREM data of Fig. 2. It is well known from dendritic growth theory that parabolic deformations may occur at the growth front as a consequence of diffusion-limited growth plus surface-tension effects.[1] In the diffusion scheme which has been proposed the continuous parabolic deformations of Fig. 2 can be interpreted as due to diffusion effects in the amorphous phase. The part played by surface tension remains unclear. It might account for the transition from the rough, "bushy" growth front in the early stages of regrowth to the continuously deformed nonplanar growth front of Fig. 2.

An estimation of the diffusion coefficient of our problem can be obtained using the theory of diffusion-controlled dendritic growth.[1] The analogy which is drawn here with liquid-solid crystallization phenomena neglects anisotropy effects. Since strong crystalline anisotropy prevails in the solid-state crystallization process, more justification is needed for the extension of the liquid-solid case beyond its validity range. In the phenomena under investigation, anisotropy manifests itself directly through the selection of deformations inclined

along ⟨111⟩ directions and indirectly through the accumulation of ⟨111⟩ stacking-fault bundles in the deformations themselves. In solid-state diffusion-controlled crystallization, crystalline anisotropy acts both through the usual anisotropy factor in the Gibbs-Thomson condition[1] and, more specifically, through an anisotropy-dependent diffusion coefficient. If the assumption is made that the diffusion coefficient is related to strain relaxations so as to allow the necessary volume change for recrystallization, it should not vary by more than an order of magnitude at most with crystalline orientation. Hence, straightforward use of the small perturbations stability theory for the plane growth front in diffusion-controlled crystallization with an anisotropy-averaged coefficient should yield a relevant order of magnitude for the length scale at which the instability occurs, as long as a small-continuous-perturbations treatment is justified. Some reassurance of the validity of such a treatment can be gained from the data shown in the electron microscopy section, where the size of the deformations and their radii of curvature were both small and of the same order. More work needs to be done on the subsequent evolution of the growth front in which the part played by strong crystalline anisotropy in nonlinear evolution is very likely to shatter the foundations on which the assumptions that have been made to treat the early stages rest, and to lead to new results.

In the liquid-solid dendritic theory, the development of diffusive instabilities resulting from the competition of the deformation favor its growth, while surface-tension effects favor its recession. The characteristic length scale λ for the development of such instabilities is provided by a planar growth-front stability analysis:[1] $\lambda \sim (d_1 l)^{1/2}$ where d_0 is the capillary length and l is the diffusion length, and $l = D/v$ with D the diffusion coefficient and v the growth-front velocity. d_0 is a microscopic length scale taken on the order of the grain size, which plays the part of lower cutoff length in our problem, $d_0 \sim 10$–20 Å. The data of Fig. 2 show that the typical size and separation of smooth deformations is 200 Å and a diffusion coefficient $D \sim 4 \times 10^{-12}$ cm^2/s can be inferred at 300 °C. It is tentatively argued that the diffusing species in the amorphous phase is a defect configuration. Dangling bonds in implanted amorphous silicon have been argued to induce SPE crystallization in this material.[22] If we compare our estimate of the diffusion constant with the low-temperature extrapolation of the diffusion coefficient for antisite configurations in GaAs, the latter falls shorter than our estimate by several orders of magnitude.[30] In this assumption of a diffusion defect, the defects would have to be highly mobile.

In GaAs, heat diffusivity is 0.4 cm^2/s and SPE growth rates are as low as 10^{-6}–10^{-7} cm/s.[21] Hence the thermal diffusion length $l = D/v$ is, by orders of magnitude, larger than the sample size so that recrystallization heat dissipation at the interface cannot be the cause of the observed instabilities. Neither is the diffusion of additional impurities introduced by ion implantation in our experiments. At 300 °C, no redistribution of implanted atoms can be observed, so that the corresponding diffusion length is much smaller than the 100-Å scale of the parabolic structures. Neither effect can account for the observations.

In summary, the first study of growth-front morphology during recrystallization of amorphous implanted GaAs films has shown two distinctive growth structures. In the initial stage of growth, the growth front is rough with an array of connected microscopic recrystallized areas. At a later stage, large continuous instabilities set in. A careful analysis of optical reflectivity has yielded an estimate of interface roughness varying as a power law with recrystallized thickness and an exponent of nearly $\frac{1}{2}$. These optical data also suggest a single mechanism to be operative in both stages of recrystallization as defined by the electron microscopy data. A mechanism based on the diffusion in the amorphous phase of defects and their reaction at the interface supports well all the experimental data. An estimate has been given for the necessary diffusion coefficient which is tentatively attributed to mobile defect configurations in the amorphous phase, whose diffusion accounts for the volume change during recrystallization. This sets an experimental and theoretical basis for this poorly understood problem of solid-phase recrystallization of III-V semiconductors.

ACKNOWLEDGMENTS

The authors would like to thank Dr. J. C. Tolédano, Dr. D. Paquet, Dr. J. M. Moison, Dr. R. Jullien, Dr. R. Botet, Dr. C. Caroli, Dr. B. Caroli, Dr. B. Roulet, and Dr. C. Misbah for enlightening discussions. The Laboratoire de Bagneux is associated with the CNRS (LA 250).

[1] J. S. Langer, Rev. Mod. Phys. **52**, 1 (1980).
[2] P. G. Saffman and G. I. Taylor, Proc. R. Soc. London, Ser. A **245**, 312 (1958).
[3] M. Eden, in *Proceedings of the Fourth Berkeley Symposium on Mathematical Statistics and Probability*, edited by F. Neyman (University of California, Berkeley, 1981), Vol. 4, p. 223.
[4] D. Richardson, Proc. Cambridge Philos. Soc. **74**, 515 (1973).
[5] T. A. Witten, Jr. and L. M. Sander, Phys. Rev. Lett. **47**, 1400 (1981).
[6] P. Meakin, Phys. Rev. Lett. **51**, 1119 (1983).
[7] M. Kolb, R. Botet, and R. Jullien, Phys. Rev. Lett. **51**, 1123 (1983).
[8] P. Meakin, Phys. Rev. B **30**, 4207 (1984).
[9] P. Ramanlal and L. M. Sander, Phys. Rev. Lett. **54**, 1828 (1985).
[10] D. A. Weitz and M. Oliveira, Phys. Rev. Lett. **52**, 1433 (1983).
[11] D. A. Weitz, J. S. Huang, M. Y. Lin, and J. Sung, Phys. Rev. Lett. **54**, 1416 (1984).
[12] P. Mangin, B. Rodmacq, and A. Chamberod, Phys. Rev. Lett. **55**, 2899 (1985).
[13] T. Vicsek, Phys. Rev. Lett. **53**, 2281 (1984); Phys. Rev. A **32**,

3084 (1985).
[14]Y. Sawada, A. Dougherty, and J. P. Gollub, Phys. Rev. Lett. **56**, 1260 (1986).
[15]D. Grier, E. Ben Jacob, R. Clarke, and L. M. Sander, Phys. Rev. Lett. **56**, 1264 (1986).
[16]E. Ben Jacob, G. Deutscher, P. Garik, N. D. Goldenfeld, and Y. Lareach, Phys. Rev. Lett. **57**, 1903 (1986).
[17]G. Radnoczi, T. Vicsek, L. M. Sander, and D. Grier (unpublished).
[18]L. Csepregi, E. F. Kennedy, J. W. Mayer, and T. W. Sigmon, Phys. Lett. **54A**, 2 (1975).
[19]K. Gamo, T. Ineda, J. W. Mayer, F. H. Eisen, and C. G. Rhodes, Radiat. Eff. **33**, 85 (1977).
[20]N. Narayan and O. W. Holland, Phys. Status Solidi A **73**, 225 (1982).
[21]C. Licoppe, Y. I. Nissim, C. Meriadec, and P. Krauz, J. Appl. Phys. **60**, 1352 (1986).
[22]G. L. Olson, S. A. Kokorowski, R. A. McFarlane, and L. D. Hess, Appl. Phys. Lett. **37**, 1019 (1980).
[23]J. G. Zabolitzky and D. Stauffer, Phys. Rev. A **34**, 1523 (1986).
[24]R. Jullien and R. Botet, J. Phys. A **18**, 2279 (1985).
[25]C. Licoppe, Y. I. Nissim, and P. Henoc, Appl. Phys. Lett. **48**, 1441 (1986).
[26]C. Licoppe, Y. I. Nissim, P. Krauz, and P. Henoc, Appl. Phys. Lett. **49**, 316 (1986).
[27]G. Müller and S. Kalbitzer, Philos. Mag. B **41**, 307 (1980).
[28]L. Csepregi, E. F. Kennedy, J. W. Mayer, and T. W. Sigmon, J. Appl. Phys. **49**, 3906 (1978).
[29]F. Spaepen and D. Turnbull, in *Laser-Solid Interactions and Laser Processing,* edited by S. D. Ferris, H. J. Leamy, and J. M. Poate (AIP, New York, 1979), p. 73.
[30]S. Makram-Ebeid, D. Gautard, P. Devillard, and G. M. Martin, Appl. Phys. Lett. **40**, 161 (1982).

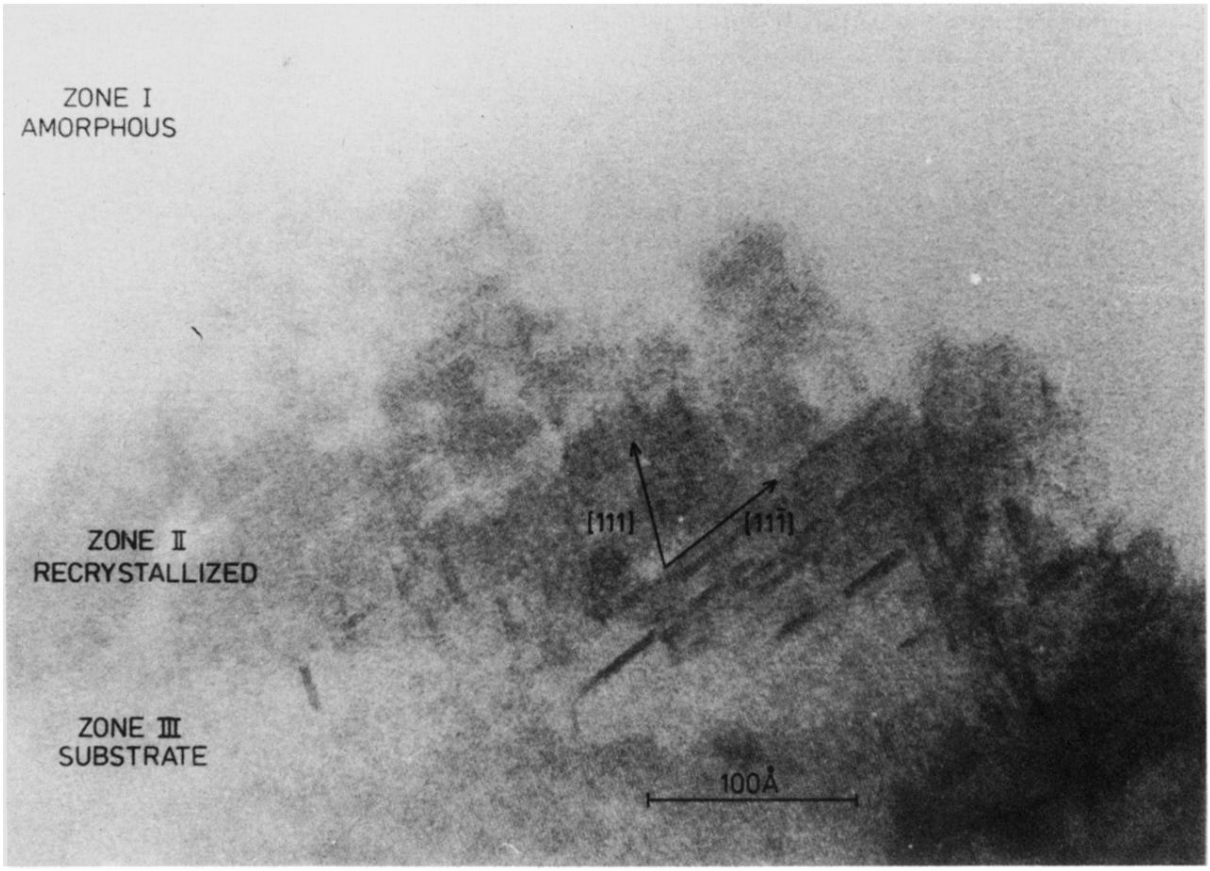

FIG. 1. HREM micrograph of the growth front after recrystallization of ~ 300 Å, showing the arborescent grain structure of the interface HREM micrograph.

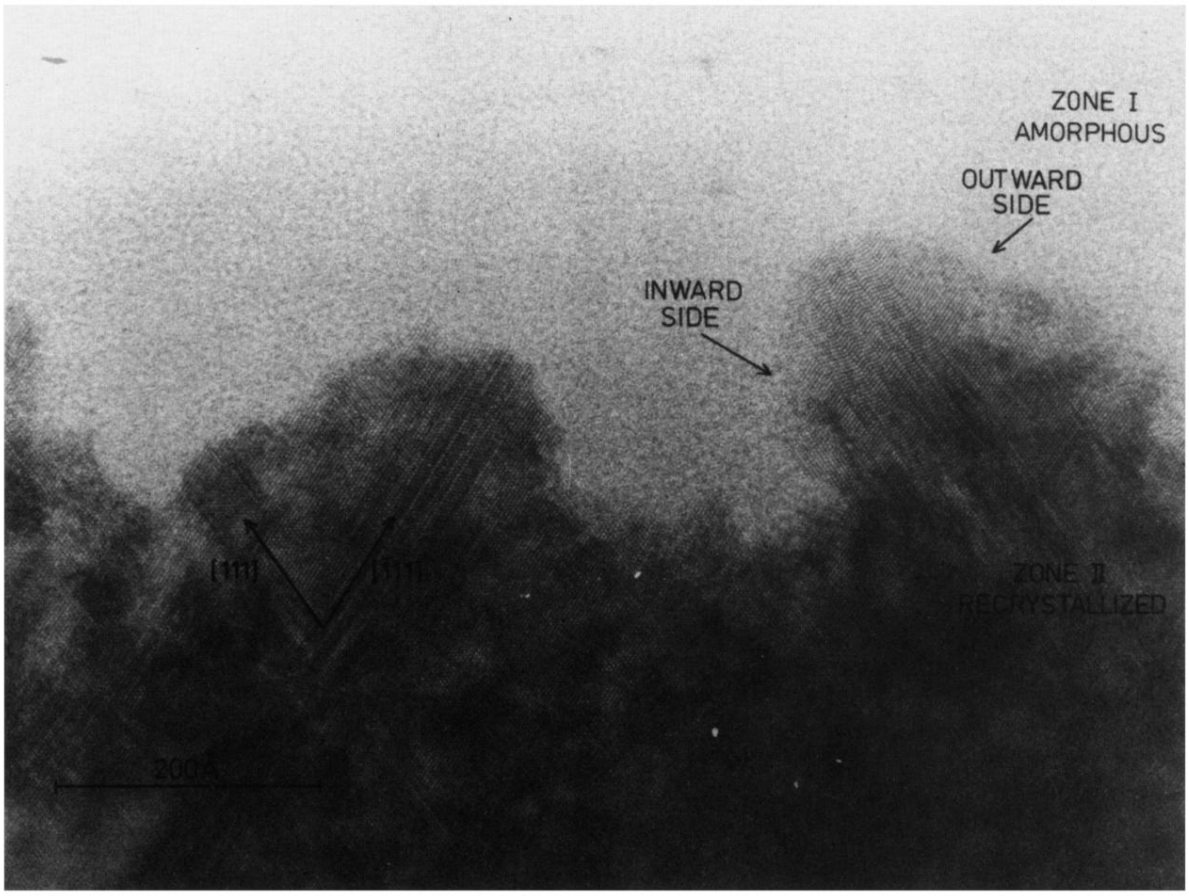

FIG. 2. HREM micrograph of the growth front after recrystallization of ~ 600 Å, showing nascent large-scale deformations protruding in [111] directions.